國立嘉義大學生命科學院

學生學術研究成果優良海報評選獲獎名單

時間:107 年 5 月 30 日

學士組

名次	獲獎人姓名	指導教師
生物資源學系		
第一名	陳俊佑	呂長澤
第二名	周紹慈	許富雄
第三名	沈芳伃	蔡若詩
微生物免疫與生物藥學系		
第一名	陳家華	朱紀實
第二名	賴純資	劉怡文
第三名	顧子奇	翁博群

微生物免疫與生物藥學系

Carbapenem-inducing resistance associated mutations in outer membrane proteins OmpK35 and OmpK36 between ESBL and non-ESBL *Klebsiella pneumoniae* isolates

Chia-Hua Chen [1], Chih-Wei Chao[1], Jen-Jain Lee [2], Chuan-Shee Liu [2], Chishih Chu [1]

[1]Department of Microbiology and Immunology and Biopharmaceuticals, National Chiayi University,
[2]Division of Infectious Diseases, Chiayi Branch, Taichung Veterans General Hospital

Background

Klebsiella pneumoniae is a Gram-negative opportunistic pathogen. Recently, an increase of carbapenem resistant isolates is associated with carbapenem treatment of ESBL- and/or AmpC-producing bacterial infection. Carbapenem-resistant is mediated through multiple mechanisms, one of the mechanisms is the insertion in outer membrane protein genes ompK35 and ompK36 by various insertion sequences. The purpose of this study is investigated the effects of different carbapenems on development of carbapenem resistance associated in ompK35 and ompK36 mutations of carbapenem-suceptible ESBL and non-ESBL producing *K. pneumoniae*.

Methods

Ten carbapenem-susceptible isolates were incubated at 2 or 0.3 µg/ml ertapenem (ETP), imipenem (IPM) and meropenem (MEM) for 36 h. Carbapenem resistant isolates were investigated for the *ompK35* and *ompK36* mutations by PCR amplification.

Results

Antibiotic susceptibility and resistant genes (Table 1)

Isolates 17 and 18 were both carbapenem intermediate and carried AmpC related gene, bla_{DHA}. All non-ESBL isolates were carbapenem sensitive except isolate 32 was IPM intermediate.

Table 1. Carbapenem susceptibility and *bla* gene of the isolates.

		ESBL					Non-ESBL			
		7	8	17	18	21	2	32	36	56	60
bla gene	bla_{DHA}	-	-	+	+	-	+	+	-	+	+
Carbapenem susceptibility	IPM	S	S	I	I	S	S	I	S	S	S
	MEM	S	S	I	I	S	S	S	S	S	S
	ETP	S	S	I	I	S	S	S	S	S	S
ESBL/AmpC		+/-	+/-	+/+	+/+	+/-	-/+	-/+	-/-	-/+	-/+

Carbapenem induction of ESBL and non-ESBL isolates (Table 2 and 3)

After 2 µg/ml IPM treatment, 37.5% (12/32), 46.8% (15/32) and 56.3% (18/32) isolates appeared resistance to IPM, MEM and ETP. 0.3 µg/ml IPM treatment induced highest resistance to ETP (65.5%, 19/29), followed by MEM (31.0%, 9/29), and IPM (27.6%, 8/29). MEM treatment could only develop resistance to ETP at 2 µg/ml. 2 µg/ml ETP treatment induced highest resistance to ETP (57.6%, 19/33), followed by MEM (39.4%, 13/33), and IPM (9.1%, 3/33). 0.3 µg/ml ETP treatment induced highest resistance to ETP (81.25%, 26/32), followed by IPM (40.6%, 13/32), and MEM (31.3%, 10/32).

After 2 µg/ml IPM and 0.3 µg/ml ETP treatment, only IPM intermediate isolate 32 developed resistance. 0.3 µg/ml IPM treatment induced highest resistance to ETP (33.3%, 3/9).. Compared that 0.3 µg/ml MEM treatment induced highest resistance to ETP (70.0%, 14/20), followed by IPM (40.0%, 8/20), and MEM (25.0%, 5/20).

Table 2. ESBL isolates resistant type after three carbapenem induction.

Carbapenem Susceptibility	Concentration of carbapenems (µg/ml)					
	2			0.3		
	Resistant to IPM / MEM / ETP					
	17	18	Total	17	18	Total
	IPM induction					
R	9/9/11	4/6/7	12/15/18	7/7/13	1/2/6	8/9/19
I	2/2/3	4/7/4	6/9/7	0/1/1	2/1/2	2/2/3
S	6/6/3	8/2/4	14/8/7	10/9/3	9/9/4	19/18/7
Total	17	15	32	17	12	29
	MEM induction					
R	0/0/1	0/0/2	0/0/3			
I	-	0/1/1	0/1/1		-	
S	1/1/0	3/2/0	4/3/0			
Total	1	3	4			
	ETP induction					
R	2/4/7	2/9/12	3/13/19	10/8/13	3/2/16	13/10/26
I	5/3/6	7/4/5	12/7/11	3/1/1	3/4/0	6/5/1
S	10/9/3	8/4/0	18/13/3	2/6/0	11/11/1	13/17/1
Total	16	17	33	15	17	32

Table 4. Non-ESBL isolates resistant type after three carbapenem induction.

Carbapenem Susceptibility	Concentration of carbapenems (µg/ml)							
	2			0.3				
	Resistant to IPM / MEM / ETP							
	32	36	Total	32	36	56	60	Total
	IPM induction							
R	2/0/2		2/0/1	1/1/1	0/0/2	-		1/1/3
I	0/1/0		0/1/0	-	2/0/0	0/1/4		2/1/4
S	1/2/1		1/2/1	1/1/1	0/2/0	5/4/1		6/7/2
Total	3		3	2	2	5		9
	MEM induction							
R			1/1/2	1/1/2	1/0/1	0/0/1		8/5/14
I		-	-	-	0/3/4	0/0/4		
S			3/3/2	3/3/2	6/4/2	5/5/0		17/15/6
Total			4	4	7	5		20
	ETP induction							
R	2/1/0	1/0/5	4/1/5	2/1/2		-		2/1/2
I	0/1/0	3/2/1	3/3/1	0/1/1		0/0/1		0/1/2
S	4/4/6	1/4/0	5/8/6	4/4/3		6/6/5	-	10/10/8
Total	6	6	12	6		6		12

54.4% of isolates were induced resistant after caebapenem treatment. ESBL isolates treat with low concentration (0.3 µg/ml) carbapenem, developed 70.0% resistant isolates. Compared to non-ESBL isolates, ESBL isolates were more easily to develop carbapenem resistance (Table 4).

Table 4. Isolates collected from carbapenem induction experiment

Concentration of antibiotics (µg/ml)	Resistant isolates / Total isolates [N, (%)]		
	ESBL	Non-ESBL	Total
2	68/124 (54.8)	10/29 (34.5)	78/153 (51.0)
0.3	85/121 (70.0)	10/44 (22.7)	95/165 (57.6)
Total	153/245 (62.4)	20/73 (27.4)	173/318 (54.4)

ompK35 and *ompK36* analysis (Table 5)

ESBL producing isolates could develop carbapenem resistance with insertion in *ompK36*. Induced resistant isolates were not found any insertion in *ompK35*. 38.3% induced resistant isolates were resistant to all carbapenems. Among these isolates, 75.0% contained normal PCR size of *ompK35* and *ompK36* that showed resistance to the carbapenem tested, demonstrating other mechanism involved in development of carbapenem resistance.

Table 5. Chang in *ompK35* and *ompK36* in 2 µg/ml carbapenem induce ESBL resistant isolates.

ompK36	*ompK35*	Antibiogram						
		MEM	ETP	IPM/ MEM	IPM/ETP	MEM/ETP	IPM/ MEM/ETP	Total [N, (%)]
M	N	2	8	1	0	4	2	17 (25.0)
N		4	16	0	2	5	24	51 (75.0)
Total [N, (%)]		6 (8.8)	24 (35.3)	1 (1.5)	2 (2.9)	9 (13.2)	26 (38.3)	68 (100.0)

M: Mutation, N: normal.

Conclusion

1. Development of carbapenem resistance depended on the isolate's carbapenem susceptibility and carbapenem types and concentration.
2. Compared to non-ESBL isolates, ESBL isolates were more easily to develop carbapenem resistance under IPM or ETP treatment.
3. Insertion sequence preferred to insertion in *ompK36*, not *ompK35*.

Combination effect of vorinostat and clinical anti-bladder cancer drugs : *in vitro* and *in vivo* study

Chun-Tzu Lai (賴純資), Pei-Min Ding (丁佩旻), and Yi-Wen Liu (劉怡文)
Department of Microbiology, Immunology and Biopharmaceuticals (DMIB), National Chiayi University, Chiayi, Taiwan

Abstract

At present, bladder cancer treatment includes surgery, chemotherapy, radiation, and immunotherapy. Surgery usually combines with chemotherapy or immunotherapy to reduce the recurrence. Among them, chemotherapy is mainly divided into intravesical and systemic administration. Mitomycin C (MMC), doxorubicin (DOXO), epirubicin, valrubicin, thiotepa and cisplatin (CP) are often used in intravesical therapy to reduce the high recurrence rate of bladder cancer and enhance the induction of cancer cells apoptosis. However, the nephrotoxicity and neurotoxicity lead to limited dose and responses. Previously, research has showed that significant histone deacetylase (HDAC) expression has been found in mouse bladder cancer animal models and human bladder cancer samples. Therefore, histone deacetylase inhibitors (HDACi) are very likely to be used in the novel treatment of bladder cancer, in combination with current anti-bladder cancer drugs, increasing their ability to cause apoptosis. Our previous study indicated that the toxicity of trichostatin A (TSA) is too high to treat bladder cancer effectively. Thus, we turned to using vorinostat (SAHA), which is also a histone deacetylation inhibitor. It was approved by the U.S. Food and Drug Administration in 2006 for the treatment cutaneous T cell lymphoma (CTCL). We aim to investigate whether vorinostat works synergistically with current bladder cancer antitumor chemotherapeutic agents and validated in vitro and in vivo study. Vorinostat and doxorubicin do have a synergistic cytotoxicity in mice bladder cancer cell MB49-Luc8. But in our in vivo study, the combination of vorinostat and doxorubicin didn't show more potent anti-bladder tumor effect. In the future, we expect to repeat the combination of vorinostat and doxorubicin in the mouse orthotopic bladder cancer model, and observe the growth rate of tumor volume by using the luminometer.

Background

➤ **Chemotherapy struggle in bladder cancer**
- Cisplatin based therapy for bladder cancer has limitations of response rate (40% to 50%), nephrotoxicity and neurotoxicity.

  Expert Review of Anticancer Therapy 2012; 12: 271.

➤ **The correlation between HDAC and bladder cancer**
- Chromatin structure modulation may be a critical step in bladder cancer progression because increased expression of HDAC-1 and 2 is linked to high grade noninvasive urothelial carcinoma.

  BMC Clinical Pathology. 2014;14:10.

➤ **HDAC inhibitor – Vorinostat**
- It is first among this new class of targeted anticancer drugs called HDAC inhibitors to be approved by the FDA for the treatment of cancer but only for cutaneous T cell lymphoma (CTCL).

- Vorinostat is more than just an alternative to established anticancer agents; it is a novel targeted anticancer drug that is selective in its effects on cancer cells.
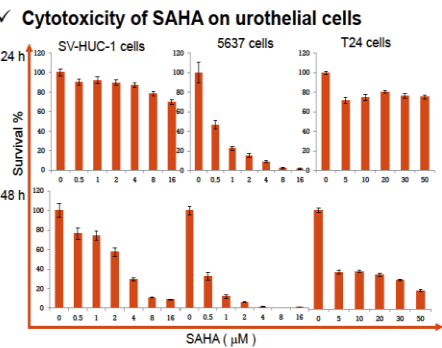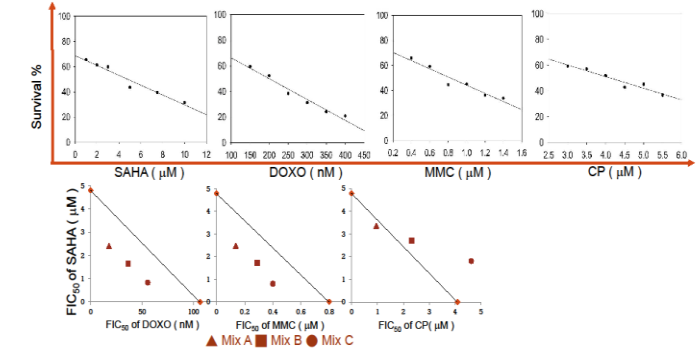
  Current Drug Metabolism, 2007;8(4):383-393.
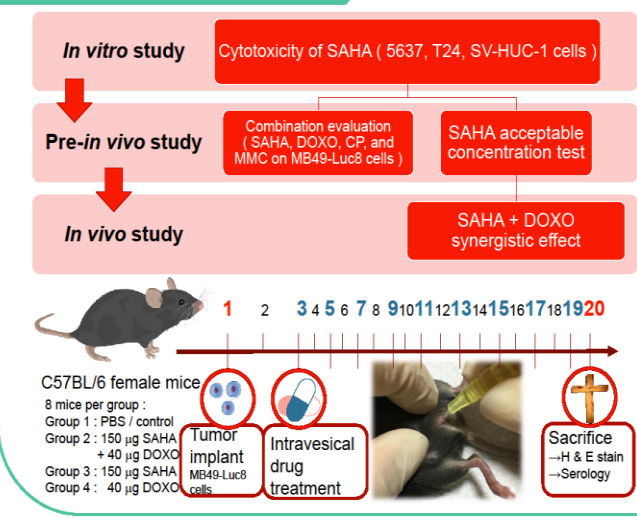
Aim

We hope to validate that the therapeutic ability of doxorubicin against bladder cancer would be enhanced synergistically by vorinostat.

Materials and Methods

In vitro study → Cytotoxicity of SAHA (5637, T24, SV-HUC-1 cells)

Pre-*in vivo* study → Combination evaluation (SAHA, DOXO, CP, and MMC on MB49-Luc8 cells) / SAHA acceptable concentration test

In vivo study → SAHA + DOXO synergistic effect

C57BL/6 female mice
8 mice per group :
Group 1 : PBS / control
Group 2 : 150 μg SAHA + 40 μg DOXO
Group 3 : 150 μg SAHA
Group 4 : 40 μg DOXO

Tumor implant MB49-Luc8 cells — Intravesical drug treatment — Sacrifice →H & E stain →Serology

Results

✓ **Cytotoxicity of SAHA on urothelial cells**

✓ **Combination of SAHA with DOXO has more synergistic effect than with MMC and with CP**

	MB49-LUC8 IC$_{50}$
Vorinostat (μM)	4.8
Doxorubicin (nM)	106.4
Cisplatin (μM)	4.1
Mitomycin C (μM)	0.8

Vorinostat combination		MB49-LUC8 CI*
Doxorubicin :	Mix A	0.670
	Mix B	0.684
	Mix C	0.695
Cisplatin :	Mix A	0.933
	Mix B	1.132
	Mix C	1.504
Mitomycin C :	Mix A	0.689
	Mix B	0.716
	Mix C	0.667

*Value less than 1 indicates synergy

✓ **No damage on mice urethelium after 50-150 μg of SAHA by intravesical treatment**
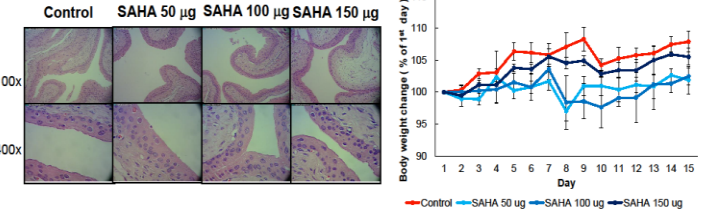
Serum biochemical data

Animal ID	Hemolysis	AST U/L	ALT U/L	BUN mg/dL	CREA mg/dL
C1	+	366.8	40.0	23.9	0.14
C2	+	193.3	41.0	26.8	0.15
50-1	+	142.8	34.3	26.9	0.17
50-3	+	146.1	36.9	25.7	0.16
100-1	+	273.9	54.4	25.2	0.14
100-2	+	201.4	58.1	31.2	0.17
100-3	+	313.1	50.1	31.2	0.22
150-1	+	636.2	57.0	25.3	0.17
150-2	+	95.6	35.2	30.0	0.18
150-3	+	175.4	56.1	27.4	0.14

Treatment description :
➤ Frequency : once every one or two days
➤ Times : 9
➤ Duration : 15 days

✓ **Combination effect of SAHA and DOXO through intravesical treatment in mouse orthotopic bladder tumor model**
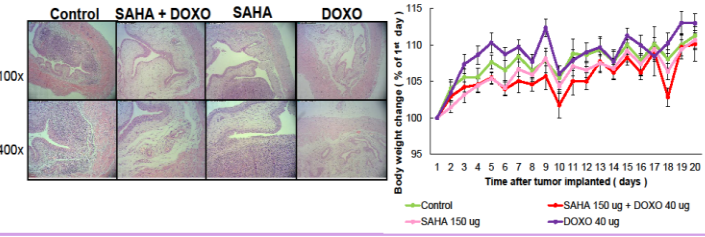
Serum biochemical data

Animal ID.	Hemolysis	AST U/L	ALT U/L	BUN mg/dL	CREA mg/dL
Control 2	+	246.7	52.1	29.1	0.28
4	+	808.7	234.8	28.9	0.29
17	+	343.1	46.7	36.0	0.26
18	+	148.9	28.4	29.8	0.27
19	+	546.9	59.0	37.5	0.36
SAHA + DOXO 20	+	114.0	65.2	39.1	0.28
5	+	166.9	28.5	22.1	0.22
6	+	412.9	45.1	35.5	0.29
7	+	86.4	32.4	31.0	0.28
8	+	113.5	28.6	33.1	0.29
21	+	99.9	60.4	35.8	0.31
22	+	264.9	70.2	42.1	0.33
23	+	265.6	67.2	34.7	0.29
24	+	219.3	61.1	42.8	0.28

Animal ID.	Hemolysis	AST U/L	ALT U/L	BUN mg/dL	CREA mg/dL
SAHA 9	+	141.4	35.3	31.9	0.30
10	+	166.9	100.4	32.6	0.32
11	+	54.8	29.0	36.6	0.25
12	+	66.8	34.9	36.0	0.28
25	+	144.8	61.6	38.1	0.23
26	+	96.7	39.0	29.5	0.22
28	+	1426.8	190.8	27.1	0.24
DOXO 14	+	83.9	35.3	30.9	0.24
15	+	82.3	31.6	28.9	0.25
16	+	70.7	29.1	31.3	0.23
29	+	99.3	39.0	37.5	0.27
30	+	211.7	98.6	32.4	0.33
31	+	344.2	60.0	39.5	0.27
32	+	255.1	37.2	29.8	0.25

Conclusion

✓ **Synergistic effect *in vitro* trial** - We identified the ability of vorinostat to synergize with doxorubicin to augment the destruction of bladder cancer cells *in vitro*.

✓ **SAHA *in vivo* trial** - Vorinostat concentration from 50 μg to 150 μg doesn't make the mice bladder markedly abnormal.

✓ **SAHA + DOXO *in vivo* trial** – Due to the tumor volume is vary from each other in group control, we couldn't make sure if the combination of vorinostat and doxorubicin had more effect than vorinostat and doxorubicin alone.

The Significances of NLR in Experimental Mouse Mammary Tumor Model

利用小鼠乳癌模式資料分析NLR在實驗小鼠腫瘤進程之關係

國立嘉義大學生命科學院 微生物免疫與生物藥學系

Department of Microbiology, Immunology and Biopharmaceuticals, College of Life Sci., National Chiayi University

Zi-Qi Gu, Yu-Ru Lai, Jia-Ying Li, Hui-Wen Chen, Wen-Yuan Xie, Xin-Yu Wang, and Bor-Chun Weng

顧子奇、賴昱儒、李佳穎、陳薈文、謝文媛、王心妤、翁博群

摘要

癌症是近代人類所面臨的難治之病症之一，而醫生在發現病人身體上有腫瘤時，可能為時已晚，因此尋找一種新興方式去提早判讀是否有罹患癌症的潛在風險顯得極為重要。在近幾年來，很多人類的臨床分析研究提到周邊血液白血球數量或比例變化可能有望成為在早期診斷腫瘤發生的快速簡便檢查方法，其中嗜中性球與淋巴球的比率(Neutrophil to lymphocyte ratio/ NLR)的改變已知與多種癌症的進程有高度的相關性，而透過分析NLR值的高低，可提供早期診斷、治療或是在預後的恢復觀察，癌症是否復發等等情形當作判斷依據，預期會更有效提升癌症的治癒。實驗小鼠作為目前實驗動物在腫瘤研究上之主流實驗動物模式，透過complete blood cells counts CBC確立周邊血液血球數據資料與腫瘤發生、癌症進程之間的相關有其必要性。本研究除了回顧分析本實驗室過去在小鼠乳癌腫瘤模式下原位癌細胞誘導小鼠的CBC歷史資料與包含腫瘤大小、白血球數量、NLR等資料的相關性做分析外，也配合高度轉移型小鼠乳癌試驗模式，進一步分析瞭解腫瘤發展進程，資料分析結果顯示NLR確實是一種新興且很好的判定癌症與否及進程的標準，此次研究也從小鼠乳癌腫瘤模式下，成功建立判定是否得癌的有效閾值。但在CBC歷史資料中顯示小鼠乳癌腫瘤模式下藥物處理也會影響NLR的高低，以免疫細胞實驗探究NLR中淋巴細胞的增生能力、T 細胞次族群的分布情形以及自然殺手細胞殺滅癌細胞的能力判斷，解釋藥物治療與影響白血球可能參與媒介腫瘤免疫的利基。

前言

目前有愈來愈多研究指出人類的腫瘤進程有著某種相關性，但對於實驗動物小鼠的NLR值卻沒有一個可以判斷的標準，誘導腫瘤及癌症的發生還是用於最傳統的方式，摸出是否有腫瘤硬塊來判斷腫瘤誘導與否，若能透過血液分析資料得知誘導成功與否，對於癌症腫瘤判斷的發生與預後將是非常有價值的，透過簡單的抽血就能得知有沒有罹癌的風險，甚至判斷其進程、是否轉移，這些都是相當重要的概念，對於往後用於臨床判斷的標準更是如此。在我們的研究中，可以明顯看到其腫瘤癌症進程確實與NLR值呈現明顯的相關性。也會以小鼠乳癌腫瘤模式下施以的藥物，觀察其對於NLR的變化對應癌症進程與對免疫細胞的影響是否有利。

材料與方法

- 使用SigmaPlot 13.0回顧性統計分析原位乳癌 (carcinoma in situ of breast/CIS) 小鼠(n=22)資料判斷NLR有無荷瘤的閾值。
- 使用由國家實驗研究院國家實驗動物中心所購買的BALB/c 雌鼠(n=15)，以高度轉移乳癌細胞(Highly metastatic breast cancer cells/HMBCCs)於第四對乳頭誘導其形成乳癌的荷瘤小鼠，Control (n=5)、PBS組(n=2)、10^5組(n=2)、4x10^5組(n=2)、 10^6組(n=2)、1.6x10^6組(n=2) 之血液資料與無處理小鼠組別回顧性資料 (n=155)共同分析NLR對於HMBCC有何意義。
- 接著誘導注射10^6的HMBCCs給BALB/c雌鼠(n=11)，再以腹腔注射施以不同藥物處理 (CP、CA、ZA)，Control (n=3)、Tumor (n=1)、Tumor + CP (n=3)、Tumor + CA (n=1)、Tumor + ZA (n=3)分析藥物作用對NLR的影響。
- 最後透過免疫細胞分離取得淋巴細胞進行淋巴細胞增生、流式細胞儀分析CD3、CD4、CD8、NK assay，探討藥物對於NLR中淋巴細胞的影響。

結果

表一、以Logistic regression回顧性統計分析原位癌小鼠，誘導前後白血球數值差異，誘導前(n=19)，誘導後(n=22)，可以發現與其他白血球資料相比不管Likelihood Ratio、Coefficient還是Odds Ratio都有較大值產生，說明NLR數值較大會有較高的機率為荷瘤狀態。在假設以75%的機率為荷瘤狀態，帶入Logit P = -6.941 + (15.433 * NLR)得出NLR閾值大約為0.5。

Details of the Logistic Regression Equation

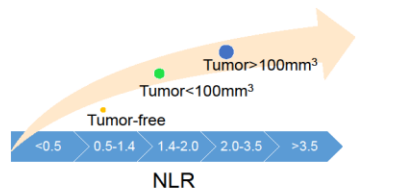|	Logit P	Likelihood Ratio (P)	Odds Ratio
WBC	-3.386 + (-0.325 * WBC)	29.424 (P <0.001)	1.384
NE	-4.451 + (1.594 * NE)	40.209 (P <0.001)	4.924
LY	-1.565 + (0.32 * LY)	5.946 (P =0.015)	1.377
MO	-3.771 + (7.687 * MO)	33.087 (P <0.001)	2180
NLR	-6.941 + (15.433 * NLR)	44.853 (P <0.001)	5040538

表二、統計資料Chi-square和Odds Ratio分析結果顯示在荷瘤狀態無論是原位乳癌還是高度轉移型乳癌細胞誘導，NLR都較正常小鼠高。有趣的是藥物處理組別也能讓NLR升高。

Statistical Analysis

	Chi-square	Odds Ratio
Carcinoma in situ	176.061 (P <0.001)	5040538
Highly metastatic breast cancer cells	186.160 (P <0.001)	632.313
Drug treatment	171.282 (P <0.001)	717.25

圖一、Chi-square結果顯示NLR值的大小(以四分位數取其間格)與腫瘤大小有關，原位乳癌細胞所誘導形成之腫瘤愈大NLR也愈大，Chi-square =176.061，P<0.001差異相當顯著。

(2a) NLR Logistic Regression in situ
(2b) NLR Logistic Regression Metastatic

圖二、(2a)回顧性統計分析原位乳癌資料的Logistic regression圖形，Y軸的0為無荷瘤；1則表示有荷瘤，無荷瘤組的NLR值集中在小於0.5的區域；荷瘤組則大多大於0.5。(2b)為HMBCCs誘導小鼠的Logistic regression圖形可以發現同樣具有明顯分區，而且NLR值與原位癌的相比，有更大的值出現。

(3a) ROC Curves in situ
(3b) ROC Curve Metastatic

圖三、(3a)回顧性統計分析原位乳癌的ROC Curve，分別以WBC, NE, LY, MO, NLR為判定條件，得到正確率最高的為NLR (A=0.99)，(3b)為HMBCCs誘導小鼠的ROC Curve，NLR (A=0.97)同樣具有有力能力檢測出小鼠有無荷瘤情形。

(4a) (4b)

圖四、(4a) HMBCCs誘導小鼠腫瘤體積積大情形。(4b) HMBCCs誘導小鼠NLR在誘導前期已然增加，後期更隨著時間繼續升高而無荷瘤小鼠NLR值則都在0.5以下。

圖五、為HMBCCs誘導小鼠經藥物處理之NLR變化圖，其中在施行藥物後的第10、12、14天發現經藥物處理組別與純荷瘤組相比NLR值有被壓低的狀況發生。
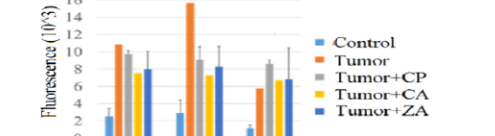
圖六、淋巴細胞增生中分別以LPS刺激B細胞、ConA刺激T細胞、HMBCCs刺激，發現荷瘤小鼠淋巴細胞增生能力較控制組好，但其中以藥物處理組別在ConA刺激下比純荷瘤組的增生能力差，說明藥物處理下NLR下降而其中淋巴細胞裡的T細胞增生能力有受藥物影響降低，而在HMBCC刺激下藥物CP組有較好的增生能力。

(7a) T helper cells (7c)
(7b) Cytotoxic cells

圖七、(7a)為Control中CD3+, CD4+的Th cells流式原圖，(7b)為Control中CD3+, CD8+的CTLs流式原圖，(7c)量化圖結果顯示不管是Th cells還是CTLs在荷瘤狀況下皆會降低比例，說明荷瘤狀態下NLR下降，其中淋巴細胞裡的T細胞比例降低，而施以藥物的三項組別比例則更低。

(8a) NK:YAC-1=E:T=1:1 (8b)

圖八、(8a)NK assay: NK:YAC-1=Effector : Target =1:1流式原圖。(8b)量化圖中 E:T=10:1結果顯示ZA組的自然殺手細胞有較好的殺滅癌細胞能力，而其NLR值的結果也是數值較低的一組。
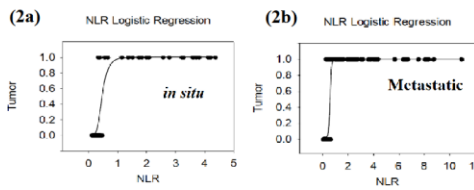
討論

回顧性統計分析原位乳癌誘導小鼠血液資料得知NLR確實是一個判斷有無荷瘤的良好判定標準，也得到其閾值NLR>0.5有高風險荷瘤機率(表一)，且與腫瘤大小相關，腫瘤愈大NLR也愈大(圖一)。進一步在高度轉移乳癌細胞(HMBCCs)誘導小鼠的實驗，進行血液分析，預期透過NLR>0.5的閾值也能判斷其有無荷瘤，得到的結果與預期是正向的，而且隨著誘導時間愈長，其NLR值甚至高過原位癌許多，進一步說明嚴重的癌症進程造成更高的NLR值產生(圖二)。而在回顧性歷史資料裡，也發現不僅荷瘤狀態會提高NLR值，以藥物處理也會造成NLR的增加(表二)，因此進行HMBCCs誘導小鼠情況下施以不同藥物處理的實驗，觀察到進行藥物處理後NLR值會被壓低(圖五)，因此認為藥物處理後可能抑制免疫細胞數量但是之後新生較快的嗜中性球與新生較慢的淋巴細胞形成較高的NLR值。淋巴細胞的各項實驗說明NLR背後淋巴細胞是如何被癌細胞、藥物處理影響，淋巴細胞增生實驗在荷瘤狀態下T細胞增生能力較強且三種藥物作用下會降低(圖六)，再透過流式細胞儀資料得出在荷瘤狀態下不管Th cells還是CTLs比例都有降低，藥物處理後更甚(圖七)，背後意涵可能為荷瘤狀態下Treg cells的比例及數量增加，造成NLR中淋巴細胞雖然總數是提升的，但是因為T細胞的各個次族群 被Treg cells抑制，造成上升比率較低，而嗜中性球則增長較快，形成NLR值持續上升的原因。而藥物方面ZA似乎有提高自然殺手細胞殺滅癌細胞的能力，造成其癌症進程較緩，也說明其NLR較其他荷瘤藥物處理組別還低的原因(圖五、圖八)。綜合以上結果顯示小鼠原位乳癌或HMBCCs模式下的NLR變化明顯回饋人類臨床回顧調查資料之結果，本次研究結果顯示NLR閾值在腫瘤免疫相關領域可以做為一個重要的試驗模式的依據。而藥物處理下也會對NLR造成影響，本次研究中以淋巴細胞實驗切入，未來會再以嗜中性球的型態、細胞表面標誌物的表達及基因表達，來解釋癌症發生時造成嗜中性球上升的原因，另一方面也積極發現能讓嗜中性球被抑制且讓淋巴細胞增生的藥物，或許能夠達到逆轉NLR值，得到提升預後存活率、降低復發、延緩癌進程的結果。
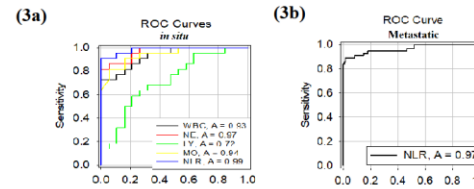
文獻探討

1. Xiaobin Gu,1 Xianshu Gao,a,1 Xiaoying Li,1 Xin Qi,1 Mingwei Ma,1 and Wen Wang1 Prognostic significance of neutrophil-to-lymphocyte ratio in prostate cancer: evidence from 16,266 patients Sci Rep. 2016; 6: 22089.
2. Coffelt S. B. et al . . IL-17-producing gammadelta T cells and neutrophils conspire to promote breast cancer metastasis. Nature, doi: 10.1038/nature14282(2015).
3. Ik Yong Kim, Sei Hwan You and Young Wan Kim Neutrophil-lymphocyte ratio predicts pathologic tumor response and survival after preoperative chemoradiation for rectal cancer BMC Surg. 2014 Nov 18;14:94.
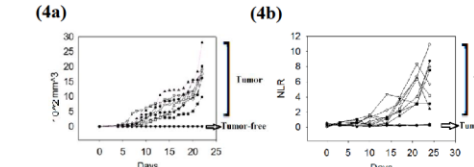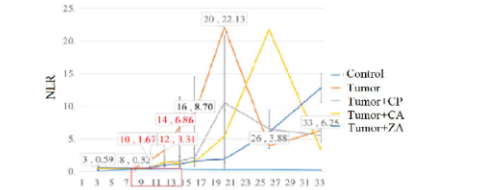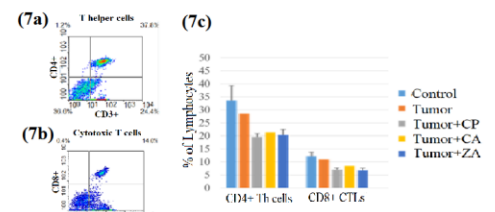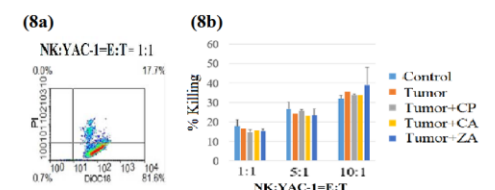
國立嘉義大學生命科學院

學生學術研究成果優良海報評選獲獎名單

時間:107 年 5 月 30 日

碩博士組

名次	獲獎人姓名	指導教師
食品科學系		
第一名	劉康佑	許成光
第二名	Nguyen Xuan Hoang(阮宣宏)	許成光
第三名	倪彥綉	吳思敬
生物資源學系		
第一名	郭晉緯	方引平
第二名	黃羽萱	方引平
第三名	李昱緯	蔡若詩
生化科技學系		
第一名	李汶鈴	陳瑞傑
第二名	黃雅晨	魏佳俐
第三名	王榆婷	魏佳俐
微生物免疫與生物藥學系		
第一名	楊芳俞	吳進益
第二名	陳德宇	謝佳雯
第三名	戴元昌	劉怡文

微生物免疫與生物藥學系

Synthesis and photocytotoxicity of 13-*O*-lipophilic substituted berberine derivatives and evaluated for their anticancer activity

Fang-Yu Yang (楊芳俞), Hong-Jhih Lin (林鴻志), Jin-Yi Wu (吳進益)*

Department of Microbiology, Immunology and Biopharmaceuticals, National Chiayi University, Chiayi, Taiwan

INTRODUCTION

Berberine is a quaternary ammonium salt from the protoberberine group of isoquinoline alkaloids. It has a wide range of biochemical and pharmacological effects. The aim of this study was to synthesize lipophilic 13-*O*-substituted berberine derivatives and to evaluate the photocytotoxic activity against two human colon cancer cell lines using MTT assay *in vitro*. In our results revealed that the longer lipophilic substituents can increase both the cellular uptake and the inhibition of cell growth on two human colon cancer cell lines. These results suggested that the presence of lipophilic substituents with moderate sizes might be crucial for the optimal anticancer and photocytotoxic activity. In conclusion, it is confirmed berberine derivatives at 13-*O*-position bearing long chain *n*-alkyl group as anticancer agents and also as potential adjuvant of photocytotoxic or chemotherapeutic drugs. The present work can be the evidence that berberine derivatives have potent anticancer photocytotoxic activities against human colon cancer cells.

MATERIALS AND METHODS

Scheme 1: Synthesis of 13-*O*-substituted berberine derivatives.

a: R = -(CH₂)₃CH₃   e: R = -(CH₂)₁₁CH₃
b: R = -(CH₂)₅CH₃   f: R = -(CH₂)₁₃CH₃
c: R = -(CH₂)₇CH₃   g: R = -(CH₂)₁₅CH₃
d: R = -(CH₂)₉CH₃   h: R = -(CH₂)₁₇CH₃
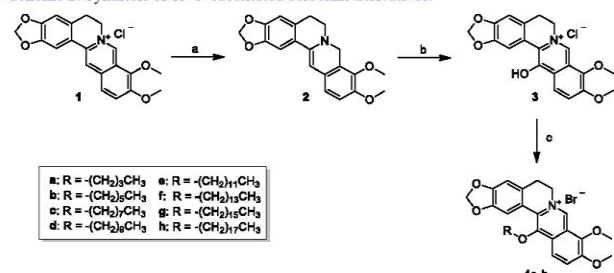
Reagents and conditions: (a) NaBH₄, K₂CO₃, MeOH, 0ºC, 2 h; (b) MCPBA, CH₂Cl₂, -20 ~ -30ºC, 2 h; then Na₂SO₃, rt, 1 h; (c) *n*-alkyl bromide, NaI, Et₃N, MeOH, reflux, 16-24 h.

RESULTS

Table 1. The IC₅₀ values and lipophilicity of berberine and its derivatives on the growth of two human colon cancer cell lines for 48 h

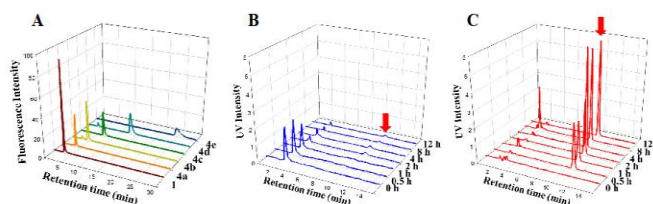| Compd	R	clog*P*	IC₅₀ (µM) SW480	IC₅₀ (µM) DLD-1
1	9-*O*-methyl	-0.77	8.22 ± 4.50	> 20
4a	13-*O*-butyl	0.95	> 20	> 20
4b	13-*O*-hexyl	2.01	2.53 ± 0.73	2.51 ± 0.74
4c	13-*O*-octyl	3.07	1.34 ± 0.03	1.24 ± 0.20
4d	13-*O*-decyl	4.12	0.77 ± 0.32	0.70 ± 0.35
4e	13-*O*-dodecyl	5.18	**0.43 ± 0.04**	**0.63 ± 0.35**
4f	13-*O*-tetradecyl	6.24	0.79 ± 0.10	0.81 ± 0.11
4g	13-*O*-cetyl	7.30	0.59 ± 0.17	0.84 ± 0.16
4h	13-*O*-octadecyl	8.36	1.58 ± 0.22	1.82 ± 0.08

Figure 1. HPLC analysis of (A) lipophilicity of compounds 1 and 4a–4e, (B) cellular uptake of 1 and (C) 4e for 0-12 h on DLD-1 cells.
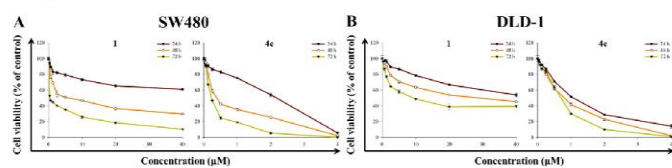

Figure 2. Cytotoxicity of (A) SW480 and (B) DLD-1 cells treated with compounds 1 and 4e.
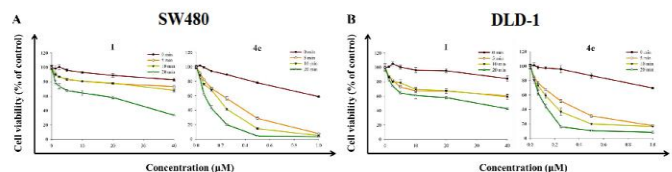

Figure 3. Dark and photocytotoxicity of (A) SW480 and (B) DLD-1 cells treated with compounds 1 and 4e after irradiation (420 nm, 5.6 mW/cm², 5, 10 and 20 min).
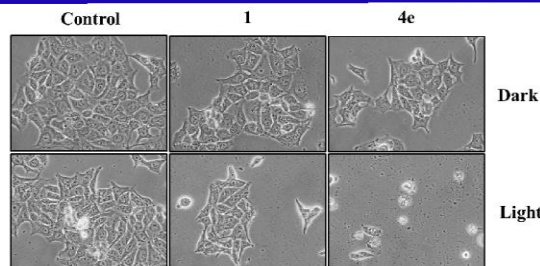

Figure 4. Cell morphological changes of DLD-1 treated with 1 (40 µM) and 4e (0.5 µM) for 24 h after irradiation.

Table 2. IC₅₀ values of compounds 1 and 4e on DLD-1 cells in the dark and after irradiation for 24 h

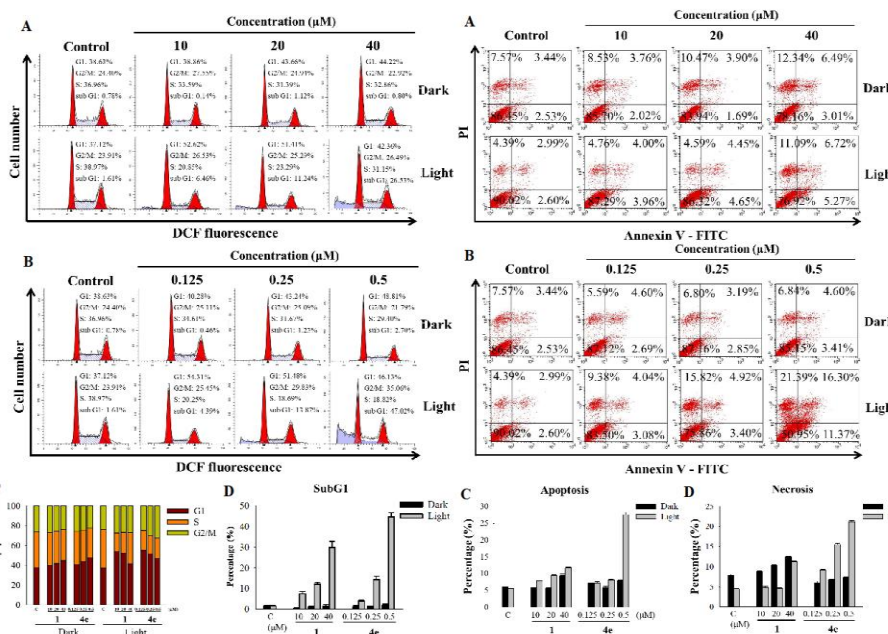| Compd	IC₅₀ (µM) SW480			IC₅₀ (µM) DLD-1		
	Dark	Light	PIF (Dark/Light)	Dark	Light	PIF (Dark/Light)
1	> 40	> 40	1.00	> 40	> 40	1.00
4e	1.47	0.20 ± 0.02	7.35	2.47 ± 0.74	0.18 ± 0.05	13.72

Figure 5. Cell cycle distribution.

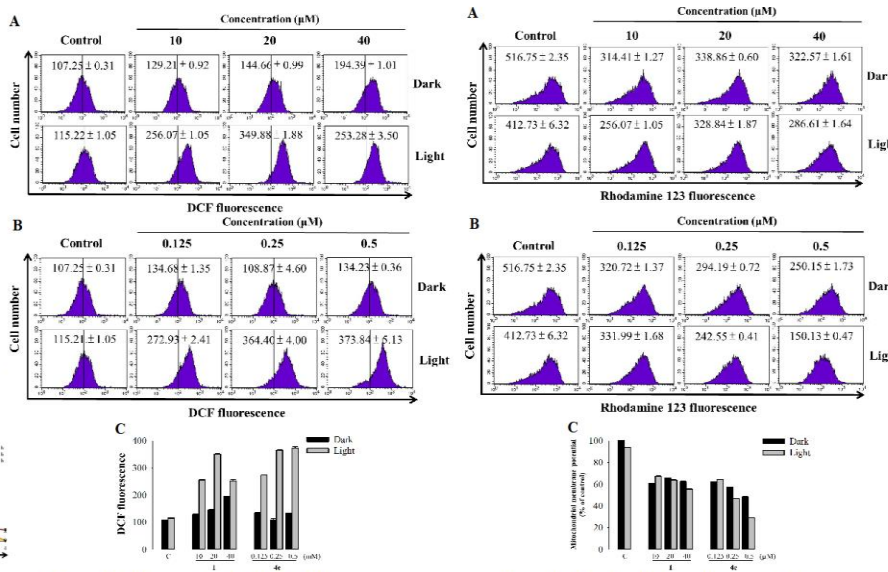**Figure 6.** Apoptosis and necrosis analysis.

Figure 7. ROS generating by DCFH-DA assay.

Figure 8. Mitochondrial membrane potential assay.

CONCLUSIONS

The introduction of long chain *n*-alkyl groups at the 13-*O*-position of berberine was to evaluate anticancer activity and the lipophilicity of berberine derivatives was analyzed by HPLC method. The photocytotoxic test confirmed that compounds 1 and 4e increased the cytotoxicity after irradiation. Vacuoles appeared in the cytoplasm after treated with compound 4e and the number of cells decreased after irradiation showed in the image and apoptotic radio proved compound 4e induce cell apoptosis after irradiation. We found that 4e increased the content of ROS generation and loss of mitochondrial membrane potential (ΔΨm) in the DLD-1 cells after visible light irradiation. In the present study, the berberine derivatives 4e can to be developed as newly photocytotoxic anticancer agent.

Characterization and improvement of solvent producing *Clostridium acetobutylicum* HOL1 on sugar utilization with mimic the lignocellulosic hydrolysates as fermentative substrate

Te-Yui Chen, Yi-Shan Yang, and Chia-Wen Hsieh*

Department of Microbiology, Immunology and Biopharmaceuticals, National Chiayi University. ∗ **Corresponding author**

Abstract

Bio-butanol is one of the bioenergy. Its production is mainly by ABE (acetone-butanol-ethanol) fermentation of *Clostridium sp.* Although most of the *Clostridium sp.* have the ability of utilizing lignocellulose as fermentative substrate, the major barrier of bio-butanol production by using lignocellulose is low xylose utilization and glucose metabolism repression on xylose. In our lab, the rapid butanol producing strain *C. acetobutylicum* HOL1 has better xylose utilization compared with parent strain. In this study, we want to figure out the mechanism of *C. acetobutylicum* HOL1 on xylose utilization and butanol production, examine the tolerance capacity of lignocellulosic hydrolysates inhibitor with mimic the lignocellulosic hydrolysates as fermentative substrate. The results showed *C. acetobutylicum* HOL1 has higher xylose utilization and butanol production on xylose and mixture of glucose and xylose. The result of metabolic gene expression level showed xylose metabolic related genes are up-regulated when xylose is present , and down-regulated when glucose is present, especially the xylose transporter. In the mixture of glucose and xylose, glucose is first depleted, while xylose is slowly utilized. The present of glucose is helpful to xylose utilization in some conditions. In lignocellulosic inhibitor tolerance experiment, *C. acetobutylicum* HOL1 has the tolerance ability compared with lignocellulosic hydrolysates inhibitor concentration in normal conditions, suggested that *C. acetobutylicum* HOL1 has its potential on using lignocellulosic hydrolysates as fermentative substrate.
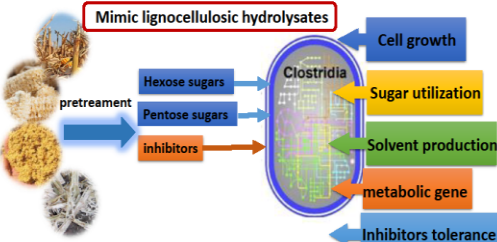
Introduction

Figure 1. Overview of mimic lignocellulosic hydrolysates as fermentation substrate of *C. acetobutylicum* HOL1
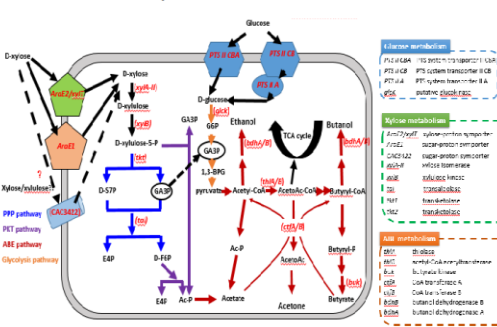

Figure 2. The gene expression of glucose, xylose and ABE metabolic pathway in *C. acetobutylicum*.
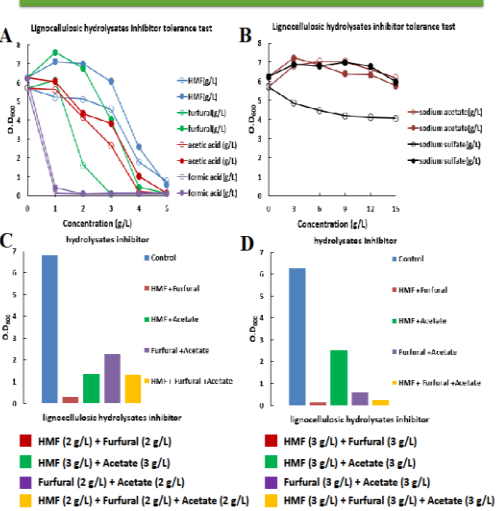
Results

Figure 3. Lignocellulosic hydrolysates inhibitors inhibit the cell growth of *C. acetobutylicum* ATCC824 and HOL1. (A) and (B) ATCC824 and HOL1 tolerance test with different concentrations of inhibitor. (C) inhibitors tolerance on ATCC824. (D) inhibitors tolerance on HOL1. Open graphic indicated ATCC824 and closed graphic indicated HOL1.

Results

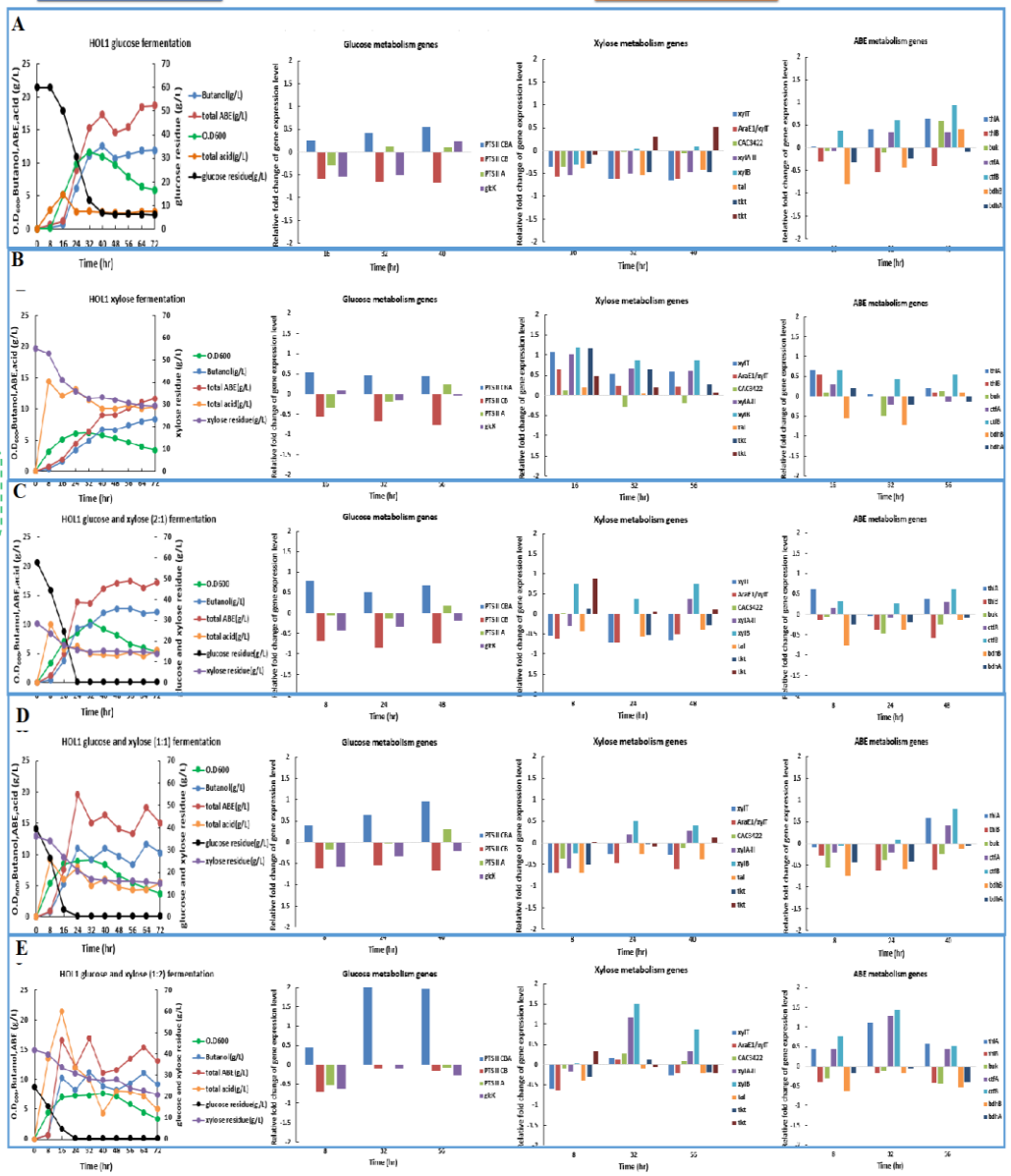### Fermentation profile

Gene expression level

Figure 4. Xylose utilization are inhibited when glucose presence and demonstrate different metabolism gene expression level. (A) glucose. (B) xylose. (C) glucose and xylose (2:1). (D) glucose and xylose (1:1). (E) glucose and xylose (1:2).

Conclusion

➢ *C. acetobutylicum* HOL1 has higher xylose utilization and butanol production on xylose and mixture of glucose and xylose, and has the tolerance ability compared with lignocellulosic hydrolysates inhibitor concentration in normal conditions

Acknowledgement

Expression of Epithelial-Mesenchymal Transition-Related Genes and their Epigenetic Regulation in Human Colorectal Cancer

Yuan-Chang Dai 戴元昌 and Yi-Wen Liu* 劉怡文*

Department of Microbiology, Immunology and Biopharmaceuticals (DMIB), National Chiayi University

Chiayi City, Taiwan

Introduction

❖ Colorectal cancer (CRC) has been the most prevalent malignancy in Taiwan for consecutive eight years.

Cancer Registry Annual Report, 2014 Taiwan. Health Promotion Administration, Ministry of Health and Welfare, Taiwan. December 2016.

❖ Despite the diversity of its etiologic and pathophysiologic factors, a biological process named as epithelial-mesenchymal transition (EMT) is indispensable in the progression of epithelial cancer.

Kim SA, et al. British Journal of Cancer 2016, 114: 199–206.
Kamimae S, et al. Oncotarget 2015, 6 (30): 29975-29990.

❖ Therefore, understanding the status of EMT and its regulation in CRC is of crucial importance and could provide novel opportunities in the treatment of CRC patients by preventing cancer progression.

Objective

❖ Our aim is to investigate the correlation of expression and methylation status of EMT-related genes with the clinicopathologic features of CRC in Taiwan, which may provide the information for prognosis evaluation and treatment prediction, as well as the potentials of these markers as therapeutic targets.

Materials and Methods

❖ Formalin-fixed and paraffin-embedded (FFPE) tumoral tissue specimens were obtained from 150 patients with CRC.

Expression of 8 EMT-related proteins (epithelial markers: E-cadherin, β-catenin, claudin-1, CD44; mesenchymal markers: N-cadherin, fibronectin, vimentin, S100A4) is explored by immunohistochemistry (IHC) and its correlation with the clinicopathologic features is assessed by statistical analysis.

❖ Using 50 paired freshly frozen tumoral and adjacent non-tumorous mucosal tissue samples, bisulfite conversion of the extracted genomic DNA with subsequent PCR, cloning and sequencing for analysis of CpG methylation level is performed on the statistically significant EMT-related markers among the proteins stated above.

Correlation between the DNA methylation status and the clinicopathologic features is then assessed by statistical analysis.

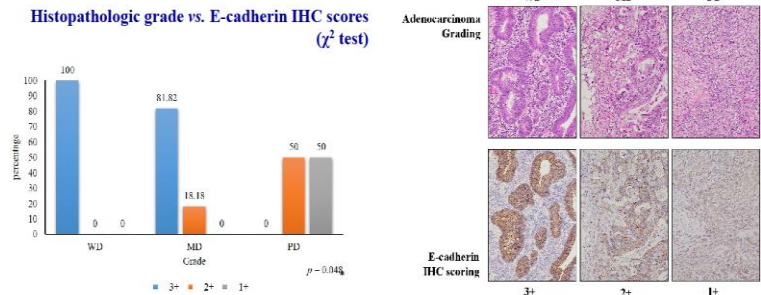❖ Genomic Data Commons Data Portal of National Cancer Institute would be mined for combined bioinformatic analysis of expression data. https://portal.gdc.cancer.gov/

Results

❖ We prospectively performed immunohistochemistry of E-cadherin, β-catenin, and vimentin on 15 CRC patients.

IHC scoring of EMT-related proteins

	0	1+	2+	3+
E-cadherin	No staining	Faint/barely perceptible incomplete membrane staining	Incomplete and/or weak/moderate membrane staining	Complete, intense circumferential membrane staining
β-Catenin	No nuclear staining	<20% nuclear staining	20~50% nuclear staining	>50% nuclear staining
Vimentin	No staining	<20% staining	20~50% staining	>50% staining

Demographic data and IHC scores

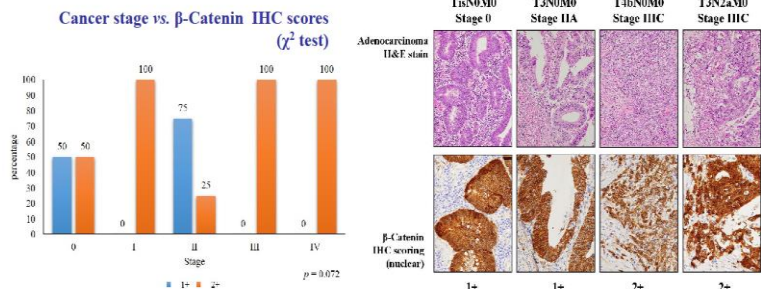| No.	Age	Gender	Location	TNM	Stage	Histologic type	Grade	ECDH	BCTN	VIM
1	70	M	Hepatic flex	Tis N0 M0	0	AIS	WD	3+	1+	0
2	81	F	Sigmoid	T3 N0 M0	II A	AD, NOS	MD	3+	1+	0
3	57	M	Descending	T4a N0 M0	II B	MUC	MD	3+	1+	0
4	68	F	Hepatic flex	T4b N0 M0	III C	AD, NOS	PD	2+	1+	0
5	62	M	Sigmoid	T4b N0 M0	III C	AD, NOS	MD	3+	2+	0
6	82	M	Ascending	T3 N1b M0	III B	AD, NOS	MD	3+	2+	0
7	79	M	Rectosigmoid	T3b N2b M0	III C	AD, NOS	MD	3+	2+	0
8	55	M	Cecum	T4a N2a M1c	IV C	SR	PD	1+	2+	3+
9	66	M	Ascending	T4b N2b M1c	IV C	AD, NOS	MD	2+	2+	0
10	74	M	Splenic flex	T4a N2a M1c	IV C	MUC	MD	3+	2+	0
11	55	M	Rectum	Tis N0 M0	0	AD, NOS	WD	3+	2+	0
12	60	F	Rectum	T1 N0 M0	I	AD, NOS	MD	3+	2+	0
13	57	M	Rectum	T2 N0 M0	I	AD, NOS	MD	3+	2+	0
14	65	M	Rectum	T3 N1a M0	III B	AD, NOS	MD	3+	2+	0
15	86	F	Rectum	T3 N2a M0	III C	AD, NOS	MD	2+	2+	0

AIS, Adenocarcinoma in situ; AD, NOS, Adenocarcinoma, not otherwise specified; MUC, Mucinous carcinoma; SIG, Signet-ring cell carcinoma; WD, Well differentiated; MD, Moderately differentiated; PD, Poorly differentiated; ECDH, E-cadherin; BCTN, β-Catenin; VIM, Vimentin.

Histopathologic grade *vs.* E-cadherin IHC scores (χ^2 test)
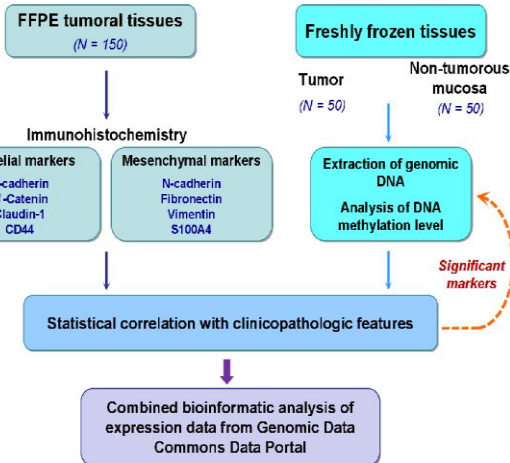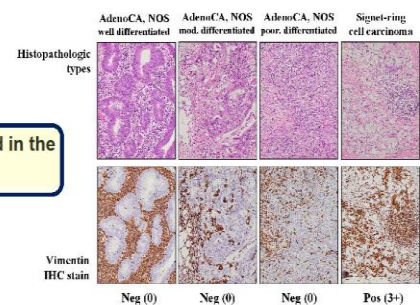
$p = 0.048$*

The expression of E-cadherin is decreased as the histopathologic grade of cancer evolving from well to poor differentiation.

Cancer stage *vs.* β-Catenin IHC scores (χ^2 test)

$p = 0.072$

The nuclear translocation of β-catenin is increased as the cancer progressing from early to advanced stage.

Vimentin is aberrantly expressed in the signet-ring cell carcinoma.

Conclusion

❖ The correlation between the immunohistochemistry scores and the histopathologic grades of colorectal cancer is statistically significant ($p = 0.048$*, χ^2 test), showing decreased E-cadherin expression as the histopathologic grade of cancer evolving from well to poor differentiation.

❖ Hence, the EMT-related protein, E-cadherin, may play a role in the progression of colorectal cancer and have the potential as a biomarker.

Future Work

❖ Completing the immunohistochemical study and the subsequent DNA methylation analysis of EMT-related markers on the predetermined cohort.

❖ Recruiting larger cohorts with long-term follow-up to evaluate the significance on tumor recurrence and patient survival.

❖ *In vitro* studies on cell lines to elucidate the underlying mechanisms.